Groundwater Potential Zone Mapping Using GIS and AHP in Eastern Nayar Watershed, Garhwal District, India

Harimohan Bhandari[1] and Ravindra K Pande[2]

Abstract

This study aims to assess the groundwater potential zones in the Eastern Nayar Watershed of the Garhwal District, Uttarakhand, utilizing GIS and AHP techniques. Various thematic layers such as land use/land cover, geology, slope, soil type, rainfall, and drainage density were integrated into a GIS environment. These layers were weighted and ranked using AHP, a multi-criteria decision-making tool. The result of the analysis revealed potential groundwater zones, providing critical insights for sustainable water resource management in the region. The study area shows only 15.74 km² with very good groundwater potential and 158.25 km² with good potential. Additionally, 272.59 km² is classified as poor, and 356.16 km² as very poor. Overall, 17.38% (173.74 km²) of the area has good groundwater potential.

Keywords: Groundwater potential, GIS, AHP, Eastern Nayar Watershed, Garhwal District, Uttarakhand, Multi-criteria analysis.

1. Introduction

Groundwater is a crucial natural resource essential for the survival and advancement of humanity. As a renewable resource, it is stored within subsurface geological formations in the earth's critical zone. It serves various purposes, including domestic, industrial, and agricultural needs, and is crucial for economic and social development in water-scarce regions (Kordestani et al., 2019).

Groundwater exists beneath the Earth's surface, filling the pore spaces of both unconsolidated and consolidated rocks, as well as the joints, fractures, and fissures of hard or crystalline rocks within the saturated zone. This water is located in the zone of saturation (ZS), where interconnected voids are filled with water. The boundary between the ZS and the zone of aeration is known as the water table. The ZS consists of various rock layers that vary in their ability to store and yield water. An aquifer is a rock formation or sequence that can store and transmit a significant amount of water. Unconfined aquifers, where groundwater is directly exposed to the atmosphere or connected through the interstitial pores of the zone of aeration, are contrasted with confined aquifers, which are isolated from the atmosphere by impermeable layers of rock or sediment.

Approximately 96.5% of Earth's water is in oceans, with groundwater making up 0.76% of total water and nearly 30% of freshwater (Eakins and Sharman, 2010). Its distribution varies spatially and temporally due to hydrogeological conditions, rainfall pattern, recharge rates, and environmental

[1] Assistant Professor (AC), Uttarakhand Open University, (Geo-informatics Department), Haldwani, (Uttarakhand), India.

[2] Former Professor, Kumaun University, (Department of Geography), Nainital, (Uttarakhand), India.

factors. Features like fractures, faults, and variations in lithology and geomorphology also affect groundwater yield, storage, transmission, and depth.

In the Himalayan region, groundwater resources face significant stress from urbanization, land use changes, over-extraction, and poor management (MacDonald et al., 2016). The impact of human activities and climate change highlights the growing importance of groundwater for food and water security (Joshi et al., 2018). Therefore, implementing Integrated Water Resources Management (IWRM) is crucial for the coordinated management of water and related resources, aiming to enhance well-being while ensuring ecosystem sustainability (Patra et al., 2018).

The Himalayan region holds nearly 20% of the world's groundwater reserves, with significant seasonal fluctuations influenced by climate, rainfall, and catchment characteristics (Pramanik et al., 2018). This groundwater is crucial during dry spells, particularly before monsoon rains (Pramanik et al., 2018). However, the rapid depletion of the Himalayan aquifer system raises concerns about agricultural sustainability and livelihoods dependent on these resources (Joshi et al., 2018). The region's rivers support various uses, including hydropower, irrigation, and municipal needs. Understanding groundwater variations in fractured terrains is essential due to the steep slopes and diverse geology (MacDonald et al., 2016). Effective groundwater management and policy development require identifying potential sites and monitoring levels, especially as irrigation is mainly managed by smallholder farmers (Joshi et al., 2018).

Groundwater is a vital resource, especially in regions where surface water is limited. The Eastern Nayar Watershed in Uttarakhand faces water scarcity, making groundwater assessment essential for sustainable management. GIS and AHP provide powerful tools for spatial analysis and decision-making in groundwater resource evaluation.

Current research shows that monsoon patterns and diverse physiographic conditions create uneven water resource distribution, causing significant shortages in some areas. During summer, many surface water sources dry up, leading agriculture to depend on groundwater from dug and shallow tube wells. Excessive and unregulated groundwater extraction has depleted these sources, harming farmers' livelihoods (Das, 2017). Therefore, accurately assessing groundwater potential is crucial for sustainable management strategies, as highlighted by the United Nations in the World Water Development Report (Connor, 2015).

A review of existing literature indicates that accurately determining groundwater potential remains a challenging task. While surface water infiltrates the earth through various penetrations and fractures, the availability of groundwater is also influenced by the characteristics and physical properties of rocks, such as porosity, permeability, and storage capacity. Additionally, several other factors, including elevation, lithology, slope, aspect, land use, river network density, faults, and soil composition, significantly contribute to groundwater availability (Rahmati et al., 2015). Furthermore, ground-based surveys and exploratory drilling methods are often both time-consuming and costly (Krishnamurthy et al., 1996).

Numerous researchers globally are utilizing remote sensing (RS) and geographical information systems (GIS) to investigate groundwater potential zones. Teeuw (1995) focused solely on lineaments for groundwater assessment, whereas other studies have integrated various factors beyond lineaments, including drainage density, geomorphology, geology, slope, land use, rainfall intensity, and soil texture (Sener et al., 2005).

Various methods have been proposed to identify groundwater potential, including geophysical (Hasan et al., 2018), hydrogeological (Amaya et al., 2018), and geological methods (Gheith and Sultan 2002). However, these often require extensive and costly field surveys and drilling. Saraf and Chaudhary (1998) demonstrated the effective use of remote sensing (RS) and geographical information systems (GIS) for groundwater exploration in the Deccan volcanic region.

The integration of remote sensing and GIS techniques has remarkably enhanced the effectiveness and accuracy of decision-making in assessing groundwater potential (Pal et al., 2020). Utilizing GIS-based Multi-Criteria Decision Analysis (MCDA) has enabled the prioritization of different parameters, with the Analytic Hierarchy Process (AHP) providing a systematic method for evaluating the significance of factors through pairwise comparisons (Saaty, 2000, 2008; Hemalatha & Kumar, 2017; Nag & Kundu, 2018; Chaudhary et al., 2021; Kumar et al., 2021b).

2. Study Area

The Eastern Nayar Watershed, located in the Garhwal District of Uttarakhand, is characterized by varied topography, moderate to high rainfall, and complex geology. Geographically, it lies between 29°45' N and 30° 8' N, and 77°40' E and 79°10' E (Figure 1).

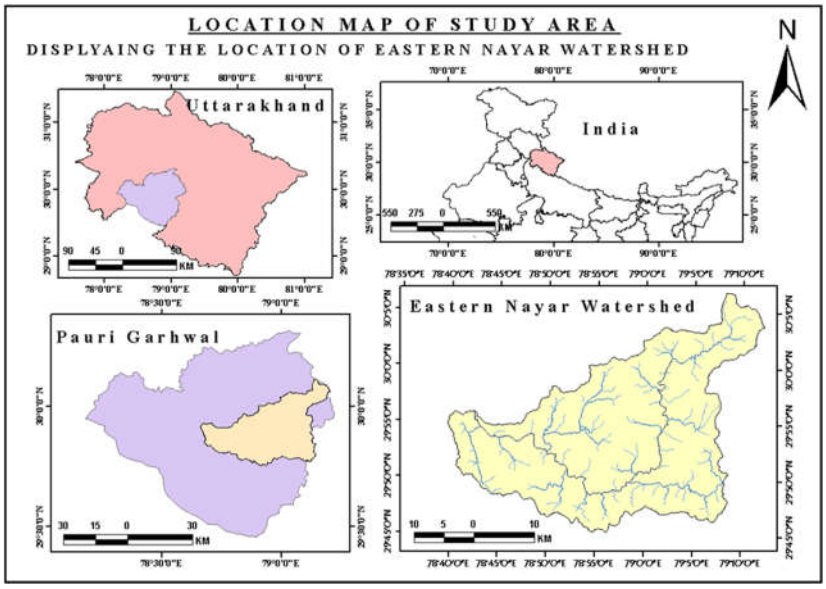

Fig. 1: Location map of the study area

The watershed encompasses a total area of 1010 km² and is located in the north-eastern part of the Garhwal District. The Eastern Nayar River, a significant tributary of the Nayar River, originates from the Dudhatoli range. It traverses a distance of 93 km from northeast to west before merging with the Western Nayar River at Satpuli, thereby forming the Nayar River. The elevation within the

watershed varies between 565 m and 3119 m above sea level (Bhandari and Mishra, 2023a). The climate in the watershed ranges from subtropical to alpine. The predominant land use and land cover types include forest, barren land, agricultural land, water bodies, and built-up areas. The watershed is an essential source of water for local communities, agriculture, and ecosystems.

3. Research Objectives:

This research aims to:

i. Identify and map groundwater potential zones.
ii. Evaluate the contribution of different factors influencing groundwater availability using GIS and AHP.
iii. Provide a reliable methodology for groundwater resource planning.

4. Material And Method

4.1. Data Collection:

The study uses satellite imagery, topographic maps, and field data for creating various thematic layers. Data on geology, land use, slope, soil type, drainage density, and rainfall were collected from remote sensing sources and ground surveys. Table 1 demonstrates various sources of data used in the present research.

Table 1: Data sources used in the study

Data	Source of data	Resolution	The Function of Data
Topographical maps	Survey of India (http://soinakshe.uk.gov. in/) (53K/9, 53K/13, 53O/1, 53N/4 and 53J/16)	1:50,000	Watershed Boundary, Natural Spring
Geological maps	https:// bhukosh.gsi.gov. in/	1:250,000	Lithology and LD Map
Landsat 8 (OLI/TIRS)	USGS (https:// earthexplorer.usgs.gov/)	30 m	LULC
Digital Elevation Model (SRTM)	USGS (https://earthexplorer.usgs.gov/)	30 m	SL, DD, and EL
Soil Map	(https://www.fao.org/soils-portal/data-hub/soil-maps-and-databases/faounesco-soil-map-of-the-world/en/)	-	Soil Map
Precipitation Map	CHRS data portal (https://chrsdata.eng.uci.edu/)	$1km^2$	Rainfall Map
Geomorphology Map	(https://bhuvan.nrsc.gov.in/home/index.php)	1:250,000	Geomorphology

4.2. Thematic Layers

The present study has utilized thematic layers obtained from both primary and secondary sources. Various thematic maps, such as those depicting geomorphology, geology, slope, lineament density, drainage density, land use/land cover, soils, and elevation, have been used to pinpoint areas with groundwater potential.

- **Geology:** Determines the permeability and porosity of rocks.

- **Slope:** Influences water infiltration rates.
- **Land Use/Land Cover (LULC):** Indicates areas of recharge and runoff.
- **Soil Type:** Affects water retention and infiltration capacity.
- **Rainfall:** Provides information on water availability for recharge.
- **Drainage Density:** A high density may limit groundwater recharge, while a low density suggests better potential.

4.3. GIS Analysis

All the thematic layers were digitized and overlaid using GIS software to identify groundwater potential zones. The methodology employed in this study is demonstrated in Figure 2.

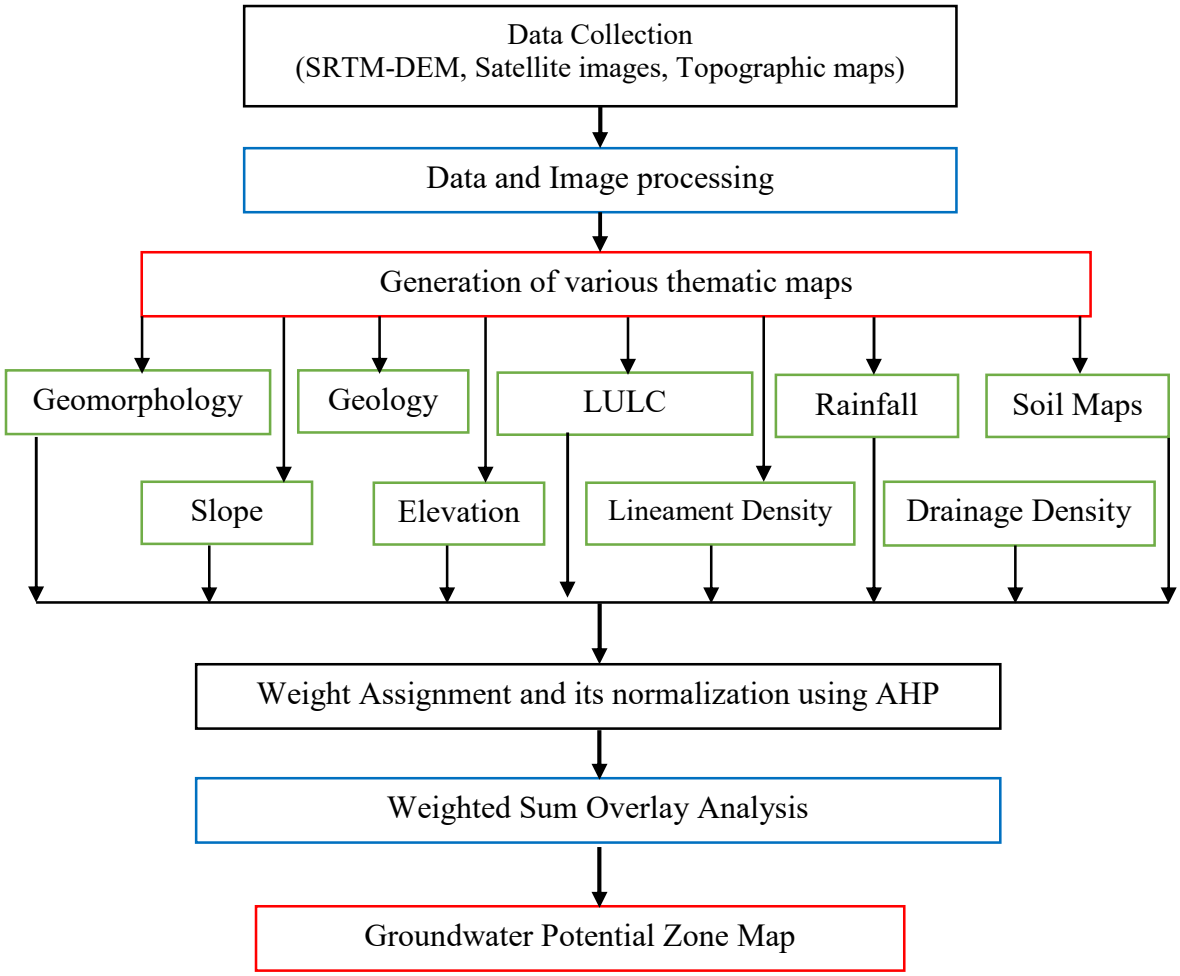

Fig. 2: Flow chart of the methodology for assessing the groundwater potential of the study area.

4.4. AHP Methodology

AHP is a widely followed effective decision-making tool proposed by Saaty depending upon the multi criteria approach (Saaty, 1980; Saaty, 2005). This approach eases the difficulty of any complex decision creation by assigning weights to different themes to formulate a hierarchical structure amongst them (Kumar and Krishna, 2018). AHP is a very powerful and robust method for multi criteria assessment by integrating domain knowledge with practical practices (Chaudhary et al.,

2010). AHP is a step by step methodical approach which includes formulation of pair wise comparison matrix (PCM) as well as normalized pair wise matrix (NPM) formulation; normalized weight computation; and consistency checking (Arulbalaji et al., 2019). The AHP technique was applied to assign weights to each thematic layer based on their relative importance in groundwater recharge. Expert judgments and pairwise comparisons were used to generate a hierarchy and calculate the consistency ratio to ensure decision reliability.

4.4.1. Pair-wise comparison matrix (PCM) Formulation

A simple however effective way to derive the interrelationship that exists between the different thematic variables is to find schematic portrayal of connection. The more powerful the influence of one thematic variable over other, the bigger it's relative importance (Dar et al., 2021). The interrelationship amongst the thematic layers was computed using Saaty's scale of relative importance on a scale of 1 to 9, where 1 demonstrates equal importance and 9 demonstrates extreme importance amongst each theme (Table 2) (Saaty, 1980; Saaty, 2005).

The Analytic Hierarchy Process (AHP), developed by Saaty in 1990, serves as a decision assistance tool frequently employed in the context of complex decision-making, particularly through pairwise comparisons. The first step in the AHP methodology involves identifying the key criteria relevant to the decision and creating a pairwise comparison matrix based on expert judgments regarding these criteria (Saaty 1990, 2005). This matrix simplifies the complex decision-making process into a single level (equation 1), enabling the calculation of comparative importance values for the criteria. The comparisons utilize Saaty's significance scale, which ranges from 1 to 9 (Table 2).

Table 2: Saaty's AHP scale of relative importance (1-9) (Saaty 1990)

Scale	1	2	3	4	5	6	7	8	9
Intensity of importance	Equal	Equal to moderate	Moderate	Equal importance	Strong	Strong to very strong	Very strong	very strong to extreme	extreme
1/9 1/8	1/7 1/6	1/5 1/4	1/3 1/2	1	2	3 4	5 6	7 8	9
← Less important				Equal importance	More important →				

Saaty's scale was utilized to characterize the different thematic variables with their relative importance and preference, which is the fundamental formulating criterion of PCM in hierarchical manner. The conceptuality of GWRPZ mapping relies on the researcher ability to establish the interrelationship between the various thematic variables in a correct manner, which can actually predict the GWR in appropriate manner (Sandoval and Tiburan, 2019).

Thus, the PCM was prepared (Equation 1) based on each thematic layer interrelationship with other thematic layer (Table 3) (Murmu et al., 2019).

$$A = [X_{ij}] \begin{vmatrix} X_{11} & X_{12} \dots & X_{1n} \\ X_{21} & X_{22} \dots & X_{2n} \\ X_{n1} & X_{n2} \dots & X_{nn} \end{vmatrix} \qquad (1)$$

Where, A is PCM; Xnn is the relative significance of a thematic variable, when compared to other parameters ; X11, X22,…, Xii, Xjj, …Xnn=1; where i, j = 1, 2,……, n; and Xij = 1/Xji;

Table 3: Pair wise comparison matrix

Parameter	RF	GM	DD	SL	LULC	LD	EL	ST	GG	Weights
Rainfall [RF]	**1**	2	3	3	4	4	5	6	7	0.309
Geomorphology [GM]	1/2	**1**	2	3	4	4	5	5	6	0.230
Drainage Density [DD]	1/3	1/2	**1**	2	3	4	4	5	6	0.164
Slope [SL]	1/3	1/3	1/2	**1**	2	3	3	4	5	0.112
Landuse [LULC]	1/4	1/4	1/3	1/2	**1**	2	3	3	4	0.080
Lineament Density [LD]	1/4	1/4	1/4	1/3	1/2	**1**	2	3	4	0.063
Elevation [EL]	1/5	1/5	1/4	1/3	1/3	1/2	**1**	2	3	0.045
Soil Type [ST]	1/6	1/5	1/5	1/4	1/3	1/3	1/2	**1**	2	0.033
Geology [GG]	1/7	1/6	1/6	1/5	1/4	1/4	1/3	1/2	**1**	0.024

4.4.2. Normalised pair wise matrix and normalized weight computation of thematic layers using AHP

In AHP formulation the next step after PCM is computation of NPM (Equation 2), where each PCM themes particular column values were divided by the corresponding column sum to obtain the NPM themes (Table 4) (Lentswe and Molwalefhe, 2020).

$$\left[C_{ij} = \frac{Y_{ij}}{Z_{ij}}\right] \qquad (2)$$

Where, Xij is NPM value at i^{st} row and j^{th} column; Y_{ij} is value at i^{th} row and j^{th} column in PCM; Zj is the column sum of j^{th} column in PCM.

From this table 4, the normalized weight for each theme computed (Equation 3) (Murmu et al., 2019; Lentswe and Molwalefhe 2020).

The sum of total row elements of a particular row divided by the number of cell in each row of NPM i.e. the total no of theme.

$$\left[W_i = \frac{\sum X_{ij}}{N}\right] \qquad (3)$$

Where, W_i is the normalized weight; N is the total number of themes.

Table 4: Normalized pair wise matrix

Parameter	RF	GM	DD	SL	LULC	LD	EL	ST	GG	Weights
Rainfall [RF]	0.31	0.41	0.39	0.28	0.26	0.21	0.21	0.20	0.18	0.309
Geomorphology [GM]	0.16	0.20	0.26	0.28	0.26	0.21	0.21	0.17	0.16	0.230
Drainage Density [DD]	0.10	0.10	0.13	0.19	0.19	0.21	0.17	0.17	0.16	0.164
Slope [SL]	0.10	0.07	0.06	0.09	0.13	0.16	0.13	0.14	0.13	0.112
Landuse [LULC]	0.08	0.05	0.04	0.05	0.06	0.10	0.13	0.10	0.11	0.080
Lineament Density [LD]	0.08	0.05	0.03	0.03	0.03	0.05	0.08	0.10	0.11	0.063
Elevation [EL]	0.06	0.04	0.03	0.03	0.02	0.03	0.04	0.07	0.08	0.045
Soil Type [ST]	0.05	0.04	0.03	0.02	0.02	0.02	0.02	0.03	0.05	0.033
Geology [GG]	0.04	0.03	0.02	0.02	0.02	0.01	0.01	0.02	0.03	0.024

4.4.3. Consistency Analysis

The most critical step associated with AHP is the consistency checking. In this procedure the principal Eigen value (λmax) calculation was done using Equations 4; 5; 6; 7; 8, which is required for consistency checking (Kumar et al., 2014).

$$A * \begin{Bmatrix} W1 \\ W2 \\ \dots \\ Wn \end{Bmatrix} \quad (4)$$

$$A' = \begin{Bmatrix} C11 & C12 \dots & C1n \\ C21 & C22 \dots & C2n \\ \dots & \dots & \dots \\ Cn1 & Cn2 \dots & Cnn \end{Bmatrix} \quad (5)$$

$$\begin{Bmatrix} C11 + C12 + \cdots + C1n \\ C21 + C22 + \cdots + C2n \\ \dots + \dots + \dots + \cdots \\ Cn1 + Cn2 + \cdots + Cnn \end{Bmatrix} = \begin{Bmatrix} S1 \\ S2 \\ \dots \\ Sn \end{Bmatrix} \quad (6)$$

$$\begin{Bmatrix} S1 \\ S2 \\ \dots \\ Sn \end{Bmatrix} \div \begin{Bmatrix} W1 \\ W2 \\ \dots \\ Wn \end{Bmatrix} = \begin{Bmatrix} Y1 \\ Y2 \\ \dots \\ Yn \end{Bmatrix} \quad (7)$$

$$\left[\lambda max = \frac{Y1+Y2+\cdots+Yn}{n}\right] \quad (8)$$

Where, A is PCM; W_1, W_2, ⋯. Wn is the normalized weight of each of the different thematic variables; A' is the matrix obtained from multiplication of PCM with normalized weight; S_1,S_2…S_n is the row sum of particular row; Y_1, Y_2⋯Y_n is the value obtained from diving S_1,S_2⋯S_n with W_1, W_2⋯W_n; n is the total number.

In the next step Consistency Index (CI) (Table 6) was calculated by using the following Equation 9.

$$\left[CI = \frac{\lambda max - 1}{n-1}\right] \quad (9)$$

Where λmaxis the principal eigenvalue, where n is the total number of thematic layers.

Maximum Eigenvector (ME) (λ_{max}) = 9.24 (n = 9)

Consistency index value (CI) = (λ_{max} – n/(n-1) = 0.03

Random index value (RI) = 1.46 (Where RI is Ratio Index (Table No.4))

Calculated consistency ratio (CR) = (CI/RI) = 0.021

Table 5: Ratio index for the different N (the number of variables) numbers, (Saaty 1990)

N	1	2	3	4	5	6	7	8	9	10
RI	0.00	0.00	0.58	0.90	1.12	1.24	1.32	1.41	1.46	1.49

Table 6: Main criteria involve in the consistency analysis of the overall evaluation

SL	Main Criteria	N	λmax	CI	RI	CR
1	Rainfall	5	5.284	0.071	1.12	0.063
2	Geomorphology	8	8.858	0.123	1.41	0.087
3	Drainage Density	5	5.133	0.033	1.12	0.03
4	Slope	5	5.284	0.070	1.12	0.062
5	Landuse	5	5.112	0.031	1.12	0.027
6	Lineament Density	5	5.117	0.029	1.12	0.026
7	Elevation	5	5.049	0.012	1.12	0.012
8	Geology	10	11.331	0.148	1.49	0.099
9	Overall Evaluation	9	9.240	0.030	1.46	0.021

Number of criteria (N), the greatest Eigenvalue of the pairwise comparison decision matrix (λmax), Consistency Index (CI), Random Inconsistency (RI) and Consistency Ratio (CR) (Saaty, 1980)

In consistency analysis, it has been found after the above procedure that CR for overall evaluation (0.021) and criterion, geomorphology (0.087), Geology (0.099), lineament density (0.026), elevation (0.012), Slope (0.062), drainage density (0.03), rainfall (0.063), and LULC (0.027), is smaller than 0.10, suggesting that the degree of consistency is reasonably acceptable (Saaty,1980) for calibration of the model. All CR values for sub-parameters are shown in Table 6 to be less than 0.10. The preferences used to generate the matrices are thus shown to be consistent.

4.5. Ranking of classes of different thematic variables

The individual thematic layer and their various features were assigned normalized weights using Saaty's analytical hierarchy process (Saaty, 1980). Each thematic layer received distinct rankings based on its importance in groundwater potential. Table 7 displays the weights assigned to the different features of each thematic layer, along with the rankings for each unit within the specific thematic layer.

Suitable ranking on a scale of five are assigned to each class (factors) of a particular thematic layer on the basis of their significance with reference to their ground water potential. The first rank classes are considered as least favourable zones for ground water exploration and fifth rank is for most potential. So, themes are classified based on their ground water potential as excellent, very good, good, moderate, poor and very poor. The final scores of each unit of the theme are equal to the product of the rank and weightage. This is calculated using raster calculator and the entire study area was quantitatively divided in to five ground water potential zones and a map showing these zones were prepared using ARC-GIS 10.8

Table 7: Ranks and weight attributed to different thematic layers

Parameter	Classes	Rank	Total Weight (%)
Rainfall (mm)	506-629 mm	1	28.4
	630-736 mm	2	
	737-833 mm	3	
	834-927 mm	4	
	928-1110 mm	5	
geomorphology	Waterbody	4	24.1
	Alluvial plain	5	
	Moderately dissected hills and valleys	3	
	Highly dissected hills and valleys	1	
	Mass wasting product	2	
	Anthropogenic terrain	1	
	Flood plain	5	
	Pediment slope	2	
Geology	Basic Rocks (Epidiorite)	1	12.9
	Diamictite, Quartzite, Slate and Boulder Bed	2	
	Gar. Mica & Chlorite Schist, Qtz with Phyllite	2	
	Granite	1	
	Grey Dolomite, Limestone, Marland Calcareous Shale	3	
	Grey Sand, Silt and Clay	5	
	Quartzite, Limestone and Occasional Conglomerate	4	

	Quartzite, Shale, Phyllite and Conglomerate	2	
	Shale With Lenticles of Limestone	2	
	Splintery Shale with Nodular Limestone	3	
Slope	0-10.8	5	13.6
	10.9-20.5	4	
	20.6-28	3	
	28.1-35.8	2	
	35.9-63.8	1	
Drainage Density	0 -0.522	5	8.9
	0.523-1.04	4	
	1.05 -1.57	3	
	1.58-2.09	2	
	1.1-2.61	1	
LULC	Agricultural land	4	4.8
	Water bodies	5	
	Forest	3	
	Barren land	2	
	Built up	1	
Lineament Density	0-0.166	1	2.8
	0.167-0.484	2	
	0.485-0.794	3	
	0.795-1.17	4	
	1.18-1.93	5	
Elevation	565-1160 m	1	2.8
	1170-1510 m	2	
	1520-1830 m	3	
	1840-2230 m	4	
	2240-3119 m	5	
Soil map	Loamy Skeletal	5	1.7
	Fine Loamy	2	

4.6. Delineation of groundwater potential zone

The groundwater Potential Index (GWPI), considering all the themes and features in an integrated layer, is calculated as:

$$GWPI = (RF_wRF_r + GM_wGM_r + DD_wDD_r + SL_wSL_r + LU_wLU_r + LD_wLD_r + EL_wEL_r + ST_wST_r + GG_wGG_r) \quad 10)$$

Where, RF is rainfall; GM is geomorphology; DD is drainage density; SL is slope; LU is Land use/land cover; LD is lineament density; EL is elevation; ST is soil type and GG is geology. Furthermore, w and r subscript represent normalized weight of a theme and rank of individual features of the theme respectively. These derived GWPI values were utilised while classifying the study area into 5 contrasting GWPZ, viz., very poor, poor, moderate, good and very good.

5. Result and Discussion

5.1. Thematic layers of the study area

5.1.1. Rainfall

Rainfall is crucial for the replenishment of groundwater resources. It influences the volume of water that seeps underground, contributing to groundwater recharge. In regions with higher rainfall,

the likelihood of groundwater replenishment increases, particularly when considering the local hydro-geological conditions (Singha et al., 2019). It is important to note that not only the total amount of rainfall matters but also the duration and intensity of the rainfall events are significant factors in the groundwater recharge process. Even small amounts of low-intensity rainfall can positively affect groundwater levels over an extended timeframe (Nasir et al., 2018). Among the variables analyzed in this study to determine Groundwater Potential Zones (GWPZs), rainfall emerged as the most significant factor, with a normalized weighting value of 0.309 (Table 4). A rainfall map for the study area was generated using the Inverse Distance Weighting (IDW) spatial interpolation method (Figure 3). The average rainfall in this area ranges from 506 to 1110 mm, predominantly occurring between July and October (Figure 3). This rainfall is categorized into five distinct classes: (i) 506 - 627 mm; (ii) 628 - 748 mm; (iii) 749 - 868 mm; (iv) 869 - 989 mm; and (v) 990 - 1110 mm. Given the direct correlation between rainfall and groundwater recharge, various classes of rainfall were assigned ranks accordingly (Table 7). Figure 3 illustrates that the south-western region experiences high rainfall, while the central area receives moderate rainfall, and the eastern and north-eastern regions have lower rainfall levels.

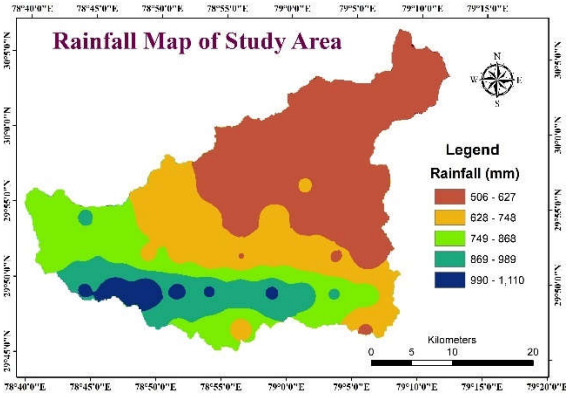

Fig. 3: Rainfall distribution

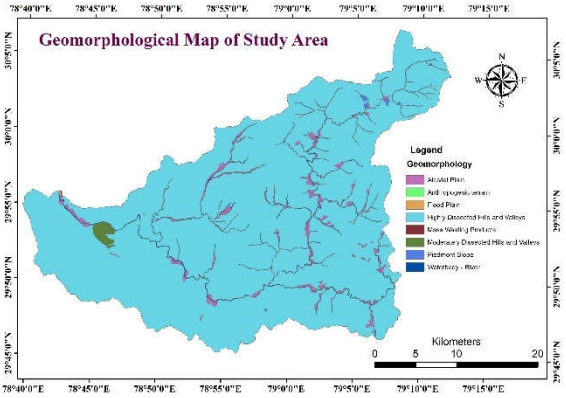

Fig. 4: Geomorphology map

5.1.2. Geomorphology

Geomorphology plays a vital role in influencing groundwater occurrence, movement, storage, percolation, and recharge within any hydro-geological province (Kumar and Krishna, 2018). This branch of physical geography focuses on the spatial distribution and characteristics of the Earth's topographical features, essentially serving as the science of landforms. Hijulstorm (1935) characterized geomorphology as the "science of landforms and land-forming processes," while Bloom (1935) described it as the "systematic description and analysis of landscapes and the processes that alter them." In the context of the Eastern Nayar watershed, geomorphology is the second most significant factor, with normalized weights of 0.230, used to identify groundwater potential zones (GWPZs). Table 7 presents the details of the geomorphology thematic layer, along with the corresponding class ranks. The watershed features highly dissected hills and valleys. The main geomorphic features in this region include water bodies, alluvial plains, moderately dissected hills and

valleys, mass wasting products, anthropogenic terrain, flood plains, and pediment slopes. A pediment is a gently sloping bedrock surface, while a pediplain is a large plain formed by merging several pediments. Among these features, alluvial and flood plains exhibit the greatest water potential, in contrast to highly dissected hills and valleys, as well as anthropogenic landscapes, which demonstrate the lowest potential (Figure 4).

5.1.3. Drainage Density

Drainage density (Dd), defined as the ratio of the total length of streams of all orders within a basin to the area of that basin, was identified as a significant morphometric parameter by Horton (1932). Dd serves as a crucial indicator of the linear dimensions of landform features in fluvial landscapes. It reflects the proximity of channel spacing, offering a quantitative assessment of the average stream channel length for the basin. This metric illustrates the drainage system's capacity to transport water across a specific area. In this analysis, drainage density values vary from 0 to 2.61 km/km². Among the selected parameters, drainage density ranks third with a normalized weight of 0.164, highlighting its relative significance in evaluating groundwater potential zones (Table 7). The classification of drainage density for groundwater recharge is as (i) 0 - 0.522 km/km²; (ii) 0.523 - 1.04 km/km²; (iii) 1.05 - 1.57 km/km²; (iv) 1.58 - 2.09 km/km²; and (v) 2.1 - 2.61 km/km² (Figure 5). It is important to note that drainage density is inversely related to permeability; thus, higher drainage density correlates with increased surface runoff and reduced groundwater reserves (Kumar and Krishna, 2018). Ranks were assigned to the drainage density classes (Table 7). Given the inverse relationship between drainage density and permeability, it is a critical element in evaluating groundwater zones. Higher drainage density values promote runoff, indicating a lower likelihood of groundwater availability. Therefore, areas with lower drainage density receive higher ranks, and vice versa. Elevated drainage density often results from less permeable subsurface materials, sparse vegetation, and significant relief. A high drainage density leads to a fine drainage texture, while a low drainage density results in a coarser texture (Strahler, 1964).

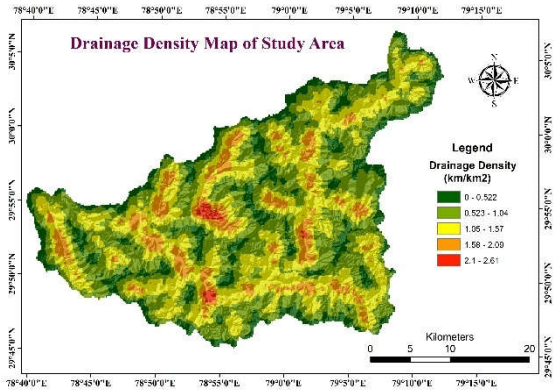

Fig. 5: Drainage density

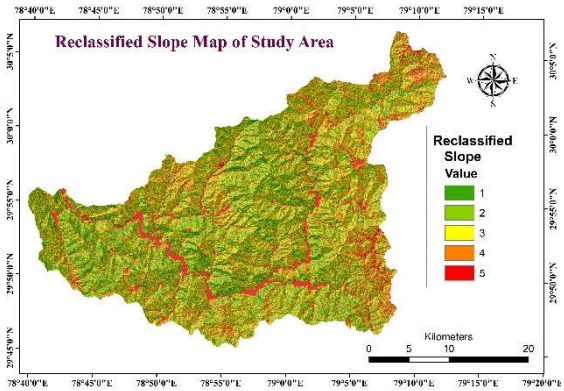

Fig. 6: Slope map

5.1.4. Slope

The slope measures elevation changes and is defined by the angle or steepness of a line, often indicating landscape steepness. There is an inverse relationship between slope and groundwater

potential: steeper slopes typically have lower groundwater potential, while flatter areas promote groundwater accumulation. Topographic slope significantly influences runoff, recharge, and surface water flow, impacting groundwater potential based on how long surface water remains before infiltration (Arulbalaji et al., 2019). Flat regions are rated very good for groundwater recharge due to high infiltration rates, while moderate slopes are good for storage, and steep slopes are poor due to increased runoff (Magesh et al., 2012). A slope map generated from SRTM DEM categorized the area into five slope ranges: 0° – 10.8°, 10.9° – 20.5°, 20.6° – 28°, 28.1° – 35.8°, and 35.9° – 63.8° (Figure 6). The analysis revealed that the lowest slope range, between 0° and 10.8°, is located in the north-eastern area, whereas slopes exceeding 35.9° are found in the southern and central hilly regions. Areas with gentler slopes were assigned higher ratings for groundwater retention, in contrast to steeper slopes, which received lower ratings due to increased runoff (Nag & Ghosh, 2013).

5.1.5. Land use /Land Cover (LULC)

Land cover refers to the diverse features present on the Earth's surface, whereas land use is associated with the human activities that occur in specific land areas. The mapping of land use and land cover is a significant application of remote sensing technology, which plays an essential role in the enhancement of groundwater resources (Waikar & Nilawar, 2014). How land is utilized is critical for groundwater recharge and the management of these resources (Sahoo et al., 2017). The interplay between land use and cover influences surface runoff through mechanisms such as evapotranspiration and infiltration, thereby affecting groundwater recharge. As a result, these land use and cover patterns have a substantial impact on the recharge of groundwater. In this research, the land use/land cover (LULC) map was assigned a normalized weight of 0.080, positioning it fifth among the parameters used to identify Groundwater Potential Zones (GWPZs) (Table 4). The ranking of land use categories, from lowest to highest potential, is as follows: built-up areas (very poor), barren land (poor), forests (moderate), water bodies (good), and agricultural land (very good) (Table 7) (Bhandari & Mishra, 2023b). Built-up areas are detrimental to groundwater recharge, reflecting the lowest potential for groundwater percolation and thus receiving the lowest rank. Conversely, water bodies demonstrate a greater capacity for groundwater percolation, achieving the highest rank, followed by agricultural land and forests.

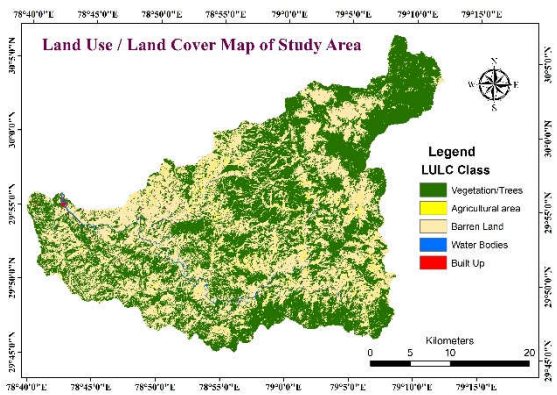

Fig. 5: LULC map

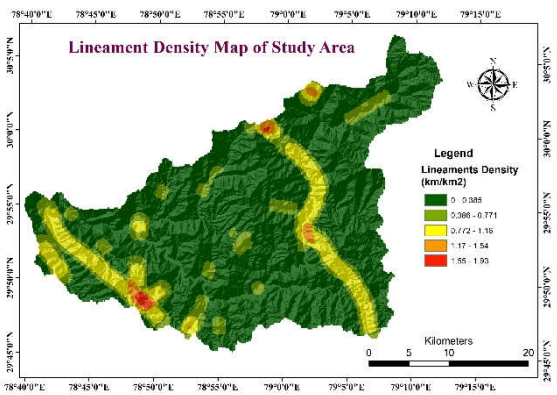

Fig. 8: Lineament density map

5.1.6. Lineament Density

Lineaments are surface expressions of underlying lithological and structural features, such as joints and faults, and are crucial for understanding groundwater resources (GWR) (O'Leary et al., 1976). They act as pathways for groundwater movement and retention, making them a key variable in hydrogeology. Identification of lineaments was achieved through satellite imagery and digital elevation models (DEM) using visual and automated techniques in ArcGIS. The observed lineaments, likely resulting from faulting and fracturing, indicate increased porosity and permeability in hard rock formations, making them significant for groundwater studies (Sreedevi et al., 2001). These geological features suggest zones of fractured bedrock with favourable groundwater conditions (Rao et al., 2001). The characteristics of the study area reveal two prominent alignments oriented in the north-south and northwest-southeast directions (Figure 8). The lineament density varies from 0 to 1.93 km/km². For this study, lineament density related to groundwater recharge has been categorized into five classes based on natural breaks: (i) 0–0.385 km/km²; (ii) 0.386–0.771 km/km²; (iii) 0.772–1.16 km/km²; (iv)1.17–1.54 km/km²; and (v) 1.55–1.93 km/km² (Figure 8). Notably, the north-eastern and south-western regions exhibit a significantly higher lineament density, while the central area shows moderate to low-density levels. A higher lineament density correlates with increased potential for water percolation, movement, storage, and occurrence (Chaudhary et al., 2019). Consequently, ranks have been assigned to the lineament density classes (Table 7).

5.1.7. Elevation

Elevation is a crucial factor in identifying areas with potential groundwater resources. In this research, a Digital Elevation Model (DEM) was employed to derive elevation data for the study region. The Eastern Nayar Watershed features a varied topography, with elevations ranging from 512 m to 3070 m above sea level. The highest elevation is found at Musa ka Kotha (3169 m), while the lowest point is located at Satpuli (569 m). Elevation is significant as the topographical altitude affects the velocity and direction of surface runoff, thereby impacting the permeability of subsurface layers (Zhang and Li, 2009). The analysis of the Eastern Nayar Watershed's contribution to groundwater potential and recharge was conducted using five elevation categories (Figure 9). The SRTM-DEM provided the necessary elevation data for the area, which was subsequently classified into five specific ranges: very low (565–1160 m), low (1170–1510 m), moderate (1520–1830 m), high (1840–2230 m), and extremely high (2240-3119 m) (Figure 9). This classification enhances the understanding and analysis of elevation differences within the research area.

5.1.8. Soil type

Soil characteristics are essential in determining how effectively surface water can seep into the groundwater system. These traits are closely associated with infiltration, percolation, and permeability rates, which affect the soil's ability to hold and allow water to infiltrate. The soil texture is a critical factor in regulating groundwater recharge (GWR) within any given hydrogeological

region (Kumar and Krishna, 2018). The composition of the soil significantly influences surface runoff and the speed at which surface water infiltrates and percolates into the subsurface, thereby impacting the area's groundwater recharge. In the study area, two main soil types have been identified: loamy skeletal and fine loamy (Figure 10). The soils have been ranked based on their infiltration rates, with the study highlighting these two textures (Figure 10). Among them, loamy skeletal soil is the most favourable for groundwater recharge, demonstrating the highest infiltration rates due to its higher sand content and more extensive interconnected pore spaces. In contrast, fine loamy soil is the least effective for GWR, as it has high clay content and limited interconnected pore spaces, hindering its infiltration capacity. It is important to note that fine loamy soil is the dominant type in the study area, making it less suitable for groundwater recharge.

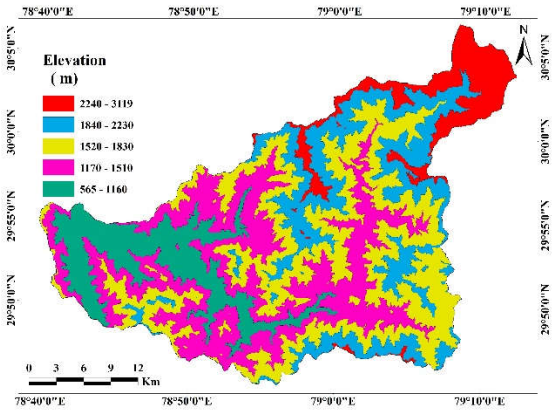

Fig. 9: Elevation map

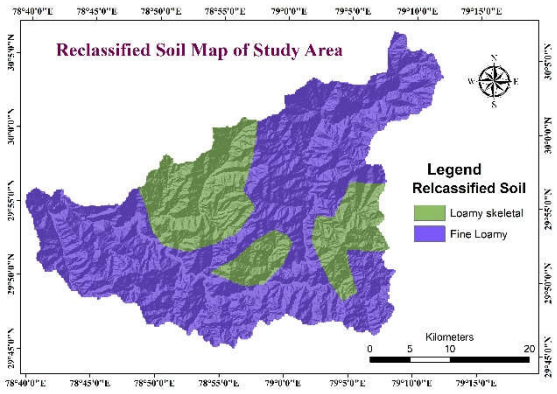

Fig. 10: Soil texture map

5.1.9. Geology

Geological characteristics are crucial in determining the infiltration and percolation of groundwater, making them an essential factor in assessing groundwater potential. The high permeability and porosity of geological units enhance groundwater storage and yield (Yildrum, 2021).

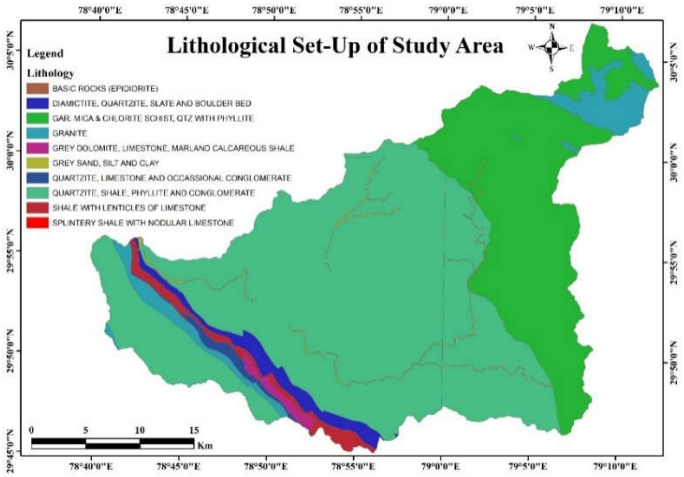

Fig.11: Lithology map of the Study Area

Furthermore, the lithological composition and its lateral and vertical variations significantly influence groundwater recharge, depending on the lithology's resistance to weathering and other

denudation processes (Kumar et al., 2021). The area under investigation is situated within the Siwalik and Middle Himalaya regions, predominantly comprising quartzite, slate, shale, and conglomerate (Figure 11). The study identifies ten distinct lithological units, including Basic Rocks (Epidiorite), Diamictite, Quartzite, Slate and Boulder Bed, Gar Mica & Chlorite Schist, Qtz with Phyllite, Granite, Grey Dolomite, Limestone, Marland Calcareous Shale, Grey Sand, Silt and Clay, Quartzite, Limestone and Occasional Conglomerate, Quartzite, Shale, Phyllite and Conglomerate, Shale with Lenticles of Limestone, and Splintery Shale with Nodular Limestone (Figure 11). The geology is the essential parameter, with the normalised weight of 0.024 adopted to ascertain the GWPG of the Eastern Nayar watershed.

5.2. Groundwater Potential Index and Validation

The GIS-based overlay analysis combined with AHP results produced a map classifying the watershed into five categories: very high, high, moderate, low, and very low groundwater potential zones (Figure 12). The study indicated that the area classified as having very good groundwater potential constitutes about 1.5% (15.74 km²) of the watershed area and is located on flat slopes adjacent to the drainage channel. The presence of very good groundwater potential in the western, central, and southeastern regions can be linked to the existence of alluvial deposits, water bodies, agricultural fields, and a high to very high lineaments density (between 1.55 and 1.93 km/km²), along with the generally flat terrain that facilitates shallow groundwater levels. The distribution of the very good GWPZ is primarily sporadic, found in the west, southeast, and certain areas of the southern part of the study area (Figure 12).

The areas identified as having good groundwater potential cover approximately 15.81% (158.25 km²) and align with geomorphic features such as moderately dissected hills and valleys, piedmont slopes, agricultural lands, water bodies, and a moderate to high lineament density (0.772 to 1.54 km/km²). In contrast, the moderate groundwater potential zones account for about 19.79% (198.10 km²) and are spread across the western, central, and southern parts of the watershed. This region is predominantly characterized by highly dissected hills, valleys, moderate to low lineament density (0.386 and 1.16 km/km²), and barren land.

Areas with poor groundwater potential cover 272.59 km², mainly on moderate to steep slopes away from major drainage systems. These zones, characterized by deep water levels, represent 27.24% of the study area and feature dissected hills, low lineament density (0.386 to 0.771 km/km²), and a mix of barren and forested lands. Regions with very low groundwater potential, primarily found in hilly areas, span 356.16 km², accounting for 35.59% of the watershed area. These areas share similar geomorphic features but have an even lower lineament density, ranging from 0 to 0.385 km/km². The results indicate that a substantial portion of the watershed is classified as having very poor groundwater potential, especially in the northern, northeastern, and eastern sections.

Groundwater potential is particularly high in proximity to river courses; however, it diminishes considerably to poor and very poor levels as the distance from these water bodies increases.

Table 8: Identification of groundwater potential zones

Sl No.	Potential Zones	Area	
		in Km^2	in %
1	Very Poor	356.16	35.59
2	Poor	272.59	27.24
3	Moderate	198.10	19.79
4	Good	158.25	15.81
5	Very Good	15.74	1.57

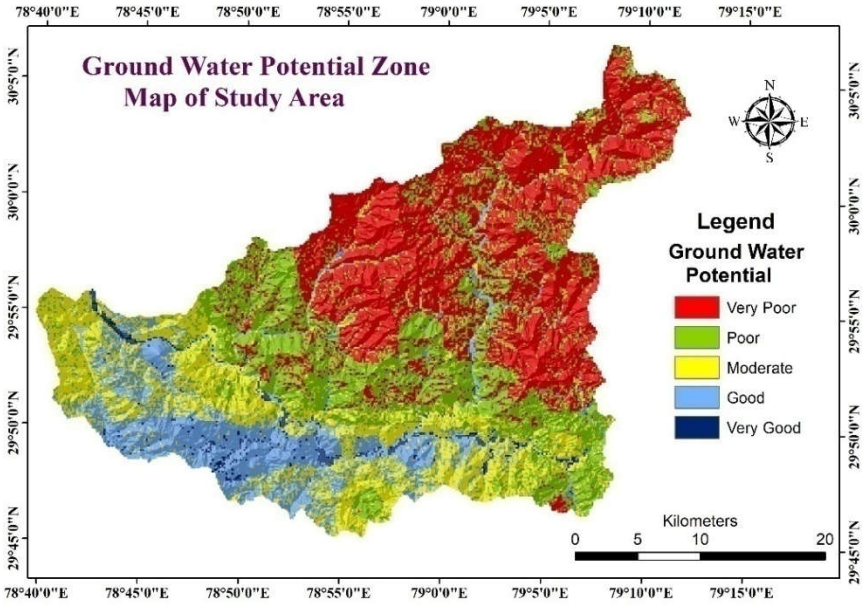

Fig.12: Potential groundwater zones map of the study area

5.2.1. Validation of GWPZ

Validation is crucial for producing groundwater potential maps from thematic layers. In this study, the locations of groundwater wells were utilized for validation purposes, integrating well and spring data with the groundwater potential map. The Receiver Operating Characteristic (ROC) curve is a standard method for validating models with high predictive accuracy, with the Area Under the Curve (AUC) serving as a key performance indicator. The ROC functions as a probability curve, while the AUC measures group separation, with correlation levels classified as poor (0.5–0.6), average (0.6–0.7), good (0.7–0.8), very good (0.8–0.9), and excellent (0.9–1) (Yesilnacar, 2005). This study collected 96 validation points (springs, wells, hand pumps) to evaluate Groundwater Potential Zones (GWPZ). The points were overlaid on the GWPZ map (Figure 14), and the Receiver Operating Characteristic (ROC) method assessed the model's accuracy (Figure 13). The ROC curve (Figure 13) showed an Area Under the Curve (AUC) of 0.745, within the 0.7 to 0.8 range, indicating a good predictive performance for the GWPZ. Therefore, field verification and well data confirmed the accuracy of the generated groundwater potential map. Areas identified as high potential showed

higher well yields, while low-potential zones corresponded to areas with minimal groundwater presence. Thus, the model is considered reasonably accurate for groundwater mapping, and the AHP model is a valuable tool for this purpose.

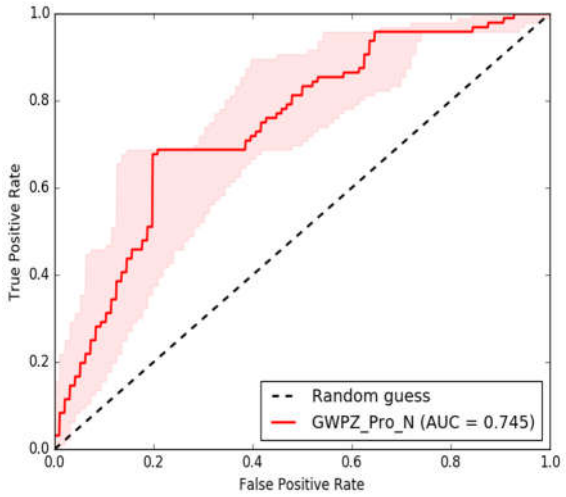

Fig.13: ROC curve for validation of GWPZ.

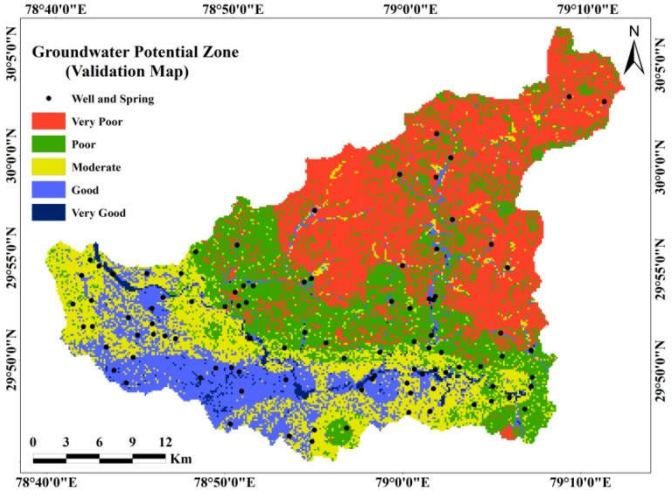

Fig. 14: Validation map of the study area.

Conclusion

Evaluating groundwater potential is an essential process for the effective and efficient utilization and management of water resources. The study assessed the groundwater potential of the Eastern Nayar watershed using an integrated GIS and AHP methodology. AHP facilitated multi-criteria decision-making on factors influencing groundwater occurrence and movement. The analysis included thematic maps of rainfall, geomorphology, drainage density, slope, land use, lineament density, elevation, soil types, and geological layers. The value assigned to each thematic layer related to groundwater potential was determined based on the outcomes of the AHP methodology. The identification of groundwater potential zones was achieved by employing weighted overlay methods to combine various thematic maps using the spatial analysis tool in ArcGIS 10.8. The resulting map categorizes groundwater potential into five distinct classes: very good potential, good potential, moderate potential, poor potential, and very poor potential. The analysis revealed that the areas classified as having good potential cover approximately 158.25 km², constituting 15.81 per cent of the total area, while those with moderate potential encompass around 198.10 km², representing 19.79 per cent. In contrast, the poor potential zones account for 27.24 per cent (272.59 km²), and the very poor potential zones cover about 356.16 km², which is equivalent to 35.59 per cent of the entire watershed.

The validity of the groundwater potential zones map was confirmed by comparing it with the distribution of wells and springs throughout the study area. The area under the curve (AUC) of the ROC analysis demonstrates a satisfactory level of accuracy for the groundwater potential zone prediction system. The findings indicate that the GWPZ map produced through the GIS-AHP integration is reliable. In a nutshell, the integration of GIS and AHP provides a robust framework for groundwater potential assessment in the Eastern Nayar Watershed. This approach can be replicated in

other regions with similar geographic and hydrological conditions. The findings will aid policymakers in making informed decisions regarding water resource management and conservation in the Garhwal District.

References

Amaya, A. G., Ortiz, J., Durán, A. and Villazon, M. (2018). "Hydrogeophysical Methods and Hydrogeological Models: Basis for Groundwater Sustainable Management in Valle Alto (Bolivia)." Sustainable Water Resources Management 5: 1–10.

Arulbalaji, P., Padmalal, D. and Sreelash, K. (2019). "GIS and AHP Techniques Based Delineation of Groundwater Potential Zones: A Case Study From Southern Western Ghats, India." Scientific Reports 9 (1): 2082.

Bhandari, H., & Mishra, M. (2023a). The Eastern Nayar Watershed: A Study Of Occupational Change. 11(3), 115–123.

Bhandari, H., & Mishra, M. (2023b). Land Use and Land Cover Change Detection Study in Eastern Nayar Watershed Using Remote Sensing and GIS. https://doi.org/10.32381/ATNAGI.2023.43.01.5

Chaudhary, A., Jha, M. K., and Chaudhary, V. M. (2010). Delineation of groundwater recharge zones and identification of artificial recharge sites in West Medinipur district, West Bengal, using RS, GIS and MCDM techniques. Environmental Earth Sciences, 59(6), pp.1209-1222.

Chaudhary, S., Kumar, A., Pramanik, M., & Negi, M. S. (2021). Land evaluation and sustainable development of ecotourism in the Garhwal Himalayan region using geospatial technology and analytical hierarchy process. *Environment, Development and Sustainability*. https:// doi. org/ 10. 1007/s10668- 021- 01528-4.

Chaudhary, A. K., Kumar, K., and Alam, M. A. (2019). Mapping of groundwater potential zones using the fuzzy analytic hierarchy process and geospatial technique. Geocarto International, pp.1-22.

Connor, R. (2015). The United Nations World Water Development Report 2015: Water for a Sustainable World. Paris: UNESCO publishing.

Dar, T., Rai, N., and Bhat, A. (2021). Delineation of potential groundwater recharge zones using analytical hierarchy process (AHP). *Geology, Ecology, and Landscapes*, *5*(4), pp.292-307.

Das, S. (2017). Delineation of groundwater potential zone in hard rock terrain in Gangajalghati block, Bankura district, India using remote sensing and GIStechniques. *Model. Earth Syst. Environ.* **3**, 1589–1599.

Eakins, B. W., and Sharman, G. F. (2010). Volumes of the World's Oceans from ETOPO1. NOAA National Geophysical Data Center, Boulder, CO, 7, p.1.

Gheith, H., and Sultan, M. (2002). "Construction of a Hydrologic Model for Estimating Wadi Runoff and Groundwater Recharge in the Eastern Desert, Egypt." Journal of Hydrology 263 (1-4): 36–55.

Golkarian A, Naghibi S. A., Kalantar, B., and Pradhan, B. (2018). Groundwater potential mapping using C5.0, random forest, and multivariate adaptive regression spline models in GIS. Environ Monit Assess. 190(3): 1–16. doi: 10.1007/s10661-018-6507-8.

Hasan, M., Shang, Y., Akhter, G. and Jin, W. (2018). "Geophysical Assessment of Groundwater Potential: A Case Study From Mian Channu Area, Pakistan." Groundwater 56 (5): 783–796.

Hemalatha, T., & Kumar, G. N. P. (2017). Multicriteria decision analysis and probabilistic modeling for evaluation in groundwater prospects. *International Journal of Advance Engineering and Research Development, 4*(8), 188–205.

Horton, R. E. (1932). Drainage-basin characteristics. Trans. Am. Geophys. Union 13, 350–361.

Joshi, S. K., Rai, S. P., Sinha, R., Gupta, S., Densmore, A. L., Rawat, Y. S., and Shekhar, S. (2018). Tracing groundwater recharge sources in the northwestern Indian alluvial aquifer using water isotopes (δ18O,δ2H and 3H). *Journal of Hydrology, 559*, 835–847. https:// doi. org/ 10. 1016/j. jhydr ol. 2018. 02. 056

Krishnamurthy, J., Venkataesa, K, N., Jayraman, V., and Manivel, M. (1996). An approach to demarcate groundwater potential zones through Remote Sensing and GIS. Internat. Jour. Remote Sensing, v.17(10), pp.1867-1884.

Kumar, A., and Krishna, A. P. (2018). Assessment of groundwater potential zones in coal mining impacted hard-rock terrain of India by integrating geospatial and analytic hierarchy process (AHP) approach. Geocarto International, 33(2), pp.105-129

Kumar, A., Pramanik, M., Chaudhary, S., & Negi, M. S. (2021b). Land evaluation for sustainable development of Himalayan agriculture using RS-GIS in conjunction with analytic hierarchy process and frequency ratio. *Journal of the Saudi Society of Agricultural Sciences, 20*(1), 1–17. https:// doi. org/ 10.1016/j. jssas. 2020. 10. 001

Kumar, M., Singh, P. and Singh, P. (2021). Fuzzy AHP based GIS and Remote Sensing techniques for the Groundwater Potential Zonation for Bundelkhand Craton Region, India. Geocarto International, (just-accepted), pp.1-21.

Kumar, T., Gautam, A. K. and Kumar, T. (2014). Appraising the accuracy of GIS-based multicriteria decision making technique for delineation of groundwater potential zones. Water resources management, 28(13), pp.4449-4466.

Lentswe, G. B., and Molwalefhe, L. (2020). Delineation of potential groundwater recharge zones using analytic hierarchy process-guided GIS in the semi-arid Motloutse watershed, eastern Botswana. J Hydrol Reg Stud 28:100674

Waikar, M. L., and Nilawar, A. P. (2014). Identification of groundwater potential zone using remote sensing and GIS technique, Int. J. Innov. Res. Sci. Eng. Technol. 3, 12163–12174.

MacDonald, A. M., Bonsor, H. C., Ahmed, K. M., Burgess, W. G., Basharat, M., Calow, R. C., Dixit, A., Foster, S. S. D., Gopal, K., Lapworth, D. J., and Lark, R. M. (2016). Groundwater quality

and depletion in the Indo-Gangetic Basin mapped from in situ observations. *Nature Geoscience, 9*(10), 762–766. https:// doi. org/ 10. 1038/ ngeo2 791

Magesh, N. S., Chandrasekar, N., and Soundranayagam, J. P. (2012). Delineation of groundwater potential zones in Theni district, Tamil Nadu, using remote sensing, GIS and MIF techniques. Geoscience Frontiers 1-8.

Murmu, P., Kumar, M., Lal, D., Sonker, I. and Singh, S.K. (2019). Delineation of groundwater potential zones using geospatial techniques and analytical hierarchy process in Dumka district, Jharkhand, India. Groundwater for Sustainable Development, 9, p.100239.

Nag, S. K., and Ghosh, P. (2013). Delineation of groundwater potential zone in Chhatna Block. Bankura District, West Bengal, India using remote sensing and GIS techniques. Environ Earth Sci.70:2115–2127.

Nag, S. K., & Kundu, A. (2018). Application of remote sensing, GIS and MCA techniques for delineating groundwater prospect zones in Kashipur block, Purulia district, West Bengal. *Applied Water Science, 8*(1), 38. https:// doi. org/ 10. 1007/ s13201- 018- 0679-9

Nasir, M., Khan, S., Zahid, H., and Khan, A. (2018). Delineation of groundwater potential zones using GIS and multi-influence factor (MIF) techniques: A study of district Swat, Khyber Pakhtunkhwa, Pakistan. Environ Earth Sci 77:367

O'leary, D. W., Friedman, J. D. and Pohn, H. A. (1976). Lineament, linear, lineation: some proposed new standards for old terms. Geological Society of America Bulletin, 87(10), pp.1463-1469.

Pal, S., Kundu, S., & Mahato, S. (2020). Groundwater potential zones for sustainable management plans in a river basin of India and Bangladesh. *Journal of Cleaner Production, 257*, 120311. https:// doi.org/ 10. 1016/j. jclep ro. 2020. 120311.

Patra, S., Mishra, P., & Mahapatra, S. C. (2018). Delineation of groundwater potential zone for sustainable development: A case study from Ganga Alluvial Plain covering Hooghly district of India using remote sensing, geographic information system and analytic hierarchy process. *Journal of Cleaner Production, 172*, 2485–2502. https:// doi. org/ 10. 1016/j. jclep ro. 2017. 11. 161

Pramanik, M. K. (2016). Site suitability analysis for agricultural land use of Darjeeling district using AHP and GIS techniques. *Modeling Earth Systems and Environment, 2*(2), 56. https:// doi. org/ 10.1007/ s40808- 016- 0116-8

Rahmati, O., Nazari, Samani, A., Mahdavi, M., Pourghasemi, H. R., & Zeinivand, H. (2015). Groundwater potential mapping at Kurdistan region of Iran using analytic hierarchy process and GIS. *Arabian Journal of Geosciences*, *8*(9), 7059–7071. https:// doi. org/ 10. 1007/ s12517- 014- 1668-4.

Rao, N. S. (2006). Groundwater potential index in a crystalline terrain using remote sensing data. Environ Geol 50:1067–1076.

Saaty, T. L. (1980). Analytic Hierarchy Process: Planning, Priority Setting, Resource Caluculation. McGrow-Hill International Book company, New York. 1−287.

Saaty, T. L. (2000). Fundamentals of decision making and priority theory with the analytic hierarchy process. RWS Publications.

Saaty, T. L. (2005). Theory and applications of the theory of the analytic network processes. Decision making with benefits, opportunities, costs, and risks. RWS Publications, Pittsburgh.

Saaty, T. L. (2008). Decision making with the analytic hierarchy process. *International Journal of Services Sciences 1*(1), 83–98.

Sahoo, S., Dhar, A., Kar, A. and Ram, P. (2017). Grey analytic hierarchy process applied to effectiveness evaluation for groundwater potential zone delineation. Geocarto International, 32(11), pp.1188-1205.

Sandoval, J. A., and Tiburan, Jr, C. L. (2019). Identification of potential artificial groundwater recharge sites in Mount Makiling Forest Reserve, Philippines using GIS and Analytical Hierarchy Process. Applied geography, 105, pp.73-85.

Saraf, A. K., & Chaudhary, P. R. (1998). Integrated remote sensing and GIS for groundwater exploration and identification of artificial recharge site. *International Journal of Remote Sensing*, *19*(10), 1825–1841

Sener, E., A. Davraz and M. Ozcelik (2005). An integration of GIS and remote Sensing in ground water Investigation: A case study in Burdur, Turkey. Hydrogeology Journal, 13: 826−834.

Singha, S. S., Pasupuleti, S., Singha, S., Singh, R. and Venkatesh, A.S. (2019). Analytic network process based approach for delineation of groundwater potential zones in Korba district, Central India using remote sensing and GIS. Geocarto International, pp.1-23.

Sreedevi, P. D., Srinivasulu, S., and Raju, K. K. (2001). Hydrogeomorphological and groundwater prospects of the Pageru river basin by using remote sensing data. Environ Geol 40:1919–1924

Teeuw, R. M. (1995). Groundwater exploration using remote sensing and a low-cost geographical information system. Hydrogeology Journal 3:21-30.

Yesilnacar, E. K. (2005). The application of computational intelligence to landslide susceptibility mapping in Turkey.

Yıldırım, U. (2021). Identification of groundwater potential zones using GIS and multi-criteria decision-making techniques: a case study upper Coruh River basin (NE Turkey). ISPRS Int J Geo-Inf 10(6):396. https:// doi. org/ 10. 3390/ ijgi1 00603 96

Zhang, Q., and Li, L. (2009). “Development and Application of an Integrated Surface Runoff and Groundwater Flow Model for a Catchment of Lake Taihu Watershed, China.” Quaternary International 208 (1-2): 102–108.